Atmos. Chem. Phys. Discuss., doi:10.5194/acp-2017-55, 2017
Manuscript under review for journal Atmos. Chem. Phys.
Discussion started: 28 February 2017

Atmospheric Chemistry and Physics Discussions

Direct radiative effects of dust aerosols emitted from the Tibetan Plateau on the East Asian summer monsoon – a regional climate model simulation

Hui Sun[1], Xiaodong Liu[1,2], and Zaitao Pan[3]

[1]SKLLQG, Institute of Earth Environment, Chinese Academy of Sciences, Xi'an, 710061, China
[2]CAS Center for Excellence in Tibetan Plateau Earth Sciences, Beijing, 100101, China
[3]Department of Earth and Atmospheric Sciences, Saint Louis University, St.Louis, Missouri, MO 63108, USA

Correspondence to: H. Sun (sunhui@ieecas.cn)

Abstract. While dust aerosols emitted from major Asian sources such as Taklimakan and Gobi Deserts have been shown to have strong effect on Asian monsoon and climate, the role of dust emitted from Tibetan Plateau (TP) itself, where aerosols can directly interact with the TP "heat pump" because of their physical proximity both in location and elevation, has not been examined. This study uses the dust coupled RegCM4.1 regional climate model to simulate the spatiotemporal distribution of dust aerosols originating in the TP and their radiative effects on the East Asian summer monsoon (EASM) during both heavy and light dust years. Two 20-year simulations with and without the dust emission from TP showed that direct radiative cooling in the mid-troposphere induced by the TP locally produced dust aerosols resulted in an overall anticyclonic circulation anomaly in the low-troposphere centered over the TP region. The northeasterly anomaly in the EASM region reduces its strength considerably. The simulations found a significant negative correlation between the TP column dust load produced by local emissions and the corresponding anomaly in the EASM index (R=−0.41). The locally generated TP dust can cause surface cooling far downstream in eastern Mongolia and northeastern China through stationery Rossby wave propagation. Although contribution to the total Asian dust source from within TP (mainly Qaidam Basin) is relatively small, its impacts on Asian monsoon and climate seems disproportionately large, likely owning to its higher elevation within TP itself.

1 Introduction

Dust is one of the most important components of atmospheric aerosols and accounts for about half of all the aerosols in the global atmosphere (Chin et al., 2002). The main source of atmospheric dust is wind erosion in arid and semi-arid regions; it is estimated that the global atmospheric dust load may be as high as 200–5000 Mt yr^{-1} (Goudie, 1983). Because of the large amount in the atmosphere, dust effects on the environment and the climate system have attracted much attention. The inhalation of dust aerosols can harm both human and animal health; it can also affect visibility and thus potentially increase the number of traffic accidents (Park and Kim, 2005). Dust aerosols also are important drivers on the

Atmos. Chem. Phys. Discuss., doi:10.5194/acp-2017-55, 2017
Manuscript under review for journal Atmos. Chem. Phys.
Discussion started: 28 February 2017

Atmospheric Chemistry and Physics Discussions

global climate because of their direct radiative effects on the Earth–atmosphere radiation balance and temperature (Tegen and Lacis, 1996; Miller et al., 2004). They can alter the atmospheric hydrological cycle by acting as cloud condensation nuclei and thus can modulate both the regional and global precipitation (Rosenfeld, 2001). Satellite observations have shown that dust originating from the Taklimakan Desert can travel around the globe within two weeks and alter the interaction between the atmospheric CO_2 and the global climate by providing nutrients to and interacting with the marine ecosystem (Uno et al., 2009).

East Asia is an important source region for dust (Zhang et al., 1996) and is home to more than half of the world's population. The lives of people in East Asia are deeply affected by the East Asian summer monsoon (EASM) and the relationship between dust aerosols and the EASM is of great interest to the scientific community. Simulations have shown that dust aerosols not only weaken the EASM (Sun et al., 2012; Guo and Yin, 2015), but can also reduce the atmospheric heat source over the Tibetan Plateau (TP) and delay the onset of the EASM (Sun et al., 2016). Aerosols, including dust aerosols, have been shown to affect the intensity of the EASM (Li et al., 2016) and variations in the EASM can modulate the spatiotemporal distribution of dust aerosols in East Asia. A recent modeling study by Lou et al. (2016) indicated that there was a negative correlation between the spring dust loading in eastern China and the East Asian monsoon.

Dust aerosols in East Asia are mainly derived from arid and semi-arid areas, including the Taklimakan Desert and the Gobi Desert. However, some studies have indicated that the TP itself may also be an important source region for dust (Zhang et al., 1996; Fang et al., 1999) and that the region is more conducive to the atmospheric transportation of dust due to its high altitude and it can interact directly with the TP thermal pump (Wu et al., 2012). However, the source and spatiotemporal distribution of dust aerosols over the TP have not been established yet. At present, there are three viewpoints about the source of dust aerosols over the TP. First, an investigation by Fang et al. (1995, 1999) showed that there exists 2047.41×10^4 km^2 of desert land over the TP, suggesting that the TP may be a potential source for dust. A numerical simulation by Chen et al. (2013) showed that dust aerosols were produced by local emissions over the TP in spring and winter. Second, satellite observations have shown that the aerosols over the TP are dominated by dust in spring and summer and that the dust aerosols were probably derived from the Taklimakan Desert and the Gubantunggut Desert to the north of the TP (Huang et al., 2007; Jia et al., 2015). Third, some studies have indicated that the dust emitted from the south of the TP, such as from the Great Indian Desert, can also be transported over the Himalaya (Lau et al., 2006, 2010).

As a massive, elevate heat source, the TP can directly heat the upper troposphere. The heating anomaly over the TP has a great impact on the EASM (Yanai and Wu, 2006; Duan et al., 2012). Studies have shown that dust aerosols over the TP can alter the local atmospheric radiation balance, affecting both the heat source over the TP and the Asian monsoon (Lau et al., 2006, 2010; Chen et al., 2013; Sun et al., 2016). However, most previous simulation studies have focused on dust aerosols originating from the Taklimakan and Gobi deserts (Zhao et al., 2006; Wang et al., 2008; Huang et al., 2009; Sun et al., 2012) and there have been few investigations of the impact of dust aerosols emitted by the TP on the East Asian

Atmos. Chem. Phys. Discuss., doi:10.5194/acp-2017-55, 2017
Manuscript under review for journal Atmos. Chem. Phys.
Discussion started: 28 February 2017

Atmospheric Chemistry and Physics Discussions

climate. The work reported here used the RegCM4.1 model to simulate climatic effects of distribution of dust aerosols surrounding the TP by performing numerical experiments with and without the emission of dust over the TP.

2 Numerical model and experiment design

2.1 RegCM4.1 model

We used the RegCM4.1 model (Regional Climate Model version 4.1), which is developed and supported by the National Center for Atmospheric Research (NCAR) and the International Center for Theoretical Physics. The model has been widely used for more than 20 years in studies of regional climatic and environmental change, especially in the simulation of the effect of aerosols on climate (Qian et al., 2003; Solomon et al., 2008; Zhang et al., 2009; Giorgi et al., 2012).

The dynamic framework of RegCM4.1 core is based on the hydrostatic core of the mesoscale model MM5 (Grell et al., 1994). The radiation scheme in RegCM4.1 is the CCM3 radiation transfer process (Kiehl et al., 1996). RegCM4.1 has two land surface process schemes: (1) the biosphere atmosphere transfer scheme (BATS1e) (Dickinson et al., 1993); and (2) the Common Land Surface process module (CLM3.5) (Oleson et al., 2008). The dust cycle can only be diagnosed when BATS1e is used. The planetary boundary layer parameterization in RegCM4.1 follows the scheme of Holtslag et al. (1990) and there are three cumulus convection parameterization schemes, including Grell (Grell et al., 1993), Kuo (Anthes, 1977) and MIT-Emmanuel (Emanuel, 1991). The dust module coupled in RegCM4.1 is based on the dust emission model (DPM) of Marticorena et al. (1995) and Alfaro and Gomes (2001). It considers dust emission, dry/wet deposition and the diagnosis of the optical and radiation characteristics of dust (including long- and short-wave radiation) (Zakey et al., 2006; Zhang et al., 2009). RegCM4.1 uses the δ-Eddington approximation for radiative flux calculations and the calculation of dust short-wave radiation uses an asymmetry factor, single scattering albedo and mass extinction coefficient based on the Mie theory. The dust long-wave radiation is accounted for by introducing the dust emissivity given by Kiehl et al. (1996).

The coupled dust module has been described in detail in previous articles (Zakey et al., 2006; Zhang et al., 2009); so only a brief introduction is given here. There are four steps in dust parameterization. First, each model grid cell is classified as either desert or non-desert according to its soil properties (such as texture, soil type, particle size and composition) based on the United States Department of Agriculture textural classification. Second, dust emission is assumed to be a function of friction velocity (u^*); dust aerosols is lifted off the ground once u^* exceeds a threshold value ($u_t^*(D_p)$).

$$u_t^*(D_p) = u_{ts}^*(D_p) \cdot f_{eff} \cdot f_w , \quad (1)$$

there $u_{ts}^*(D_p)$ depends on soil particle size(D_p), f_{eff} and f_w are the correction terms for nonerodible surface roughness elements (Marticorena and Bergametti, 1995) and soil moisture content (Fecan et al., 1999), respectively.

Atmos. Chem. Phys. Discuss., doi:10.5194/acp-2017-55, 2017
Manuscript under review for journal Atmos. Chem. Phys.
Discussion started: 28 February 2017

Atmospheric Chemistry and Physics Discussions

Third, the horizontal mass flux is treated as a function of the frictional velocity and is given by:

$$dH_F(D_p) = E \cdot \frac{\rho_a}{g} \cdot u^{*3} \cdot (1 + R(D_p)) \cdot (1 - R^2(D_p)) \cdot dS_{rel}(D_p), \quad (2)$$

where E, ρ_a and g are the ratio of the erodible to total surface areas, the surface air density and the gravitational acceleration, respectively. $R(D_p)$ is the ratio of the threshold frictional velocity in equation (1) to the frictional velocity u^* calculated within each grid cell from the model prognostic surface wind and surface roughness height. $dS_{rel}(D_p)$ is the relative surface area of a soil aggregate of diameter D_p to the total surface area of soil aggregates. The vertical flux corresponding to each emission mode is calculated by:

$$F_{dust,i}(D_p) = (\frac{\pi}{6}) \cdot \rho_p \cdot D_i^3 \cdot N_i, \quad (3)$$

where ρ_p is the aggregate density (2.65 g cm^{-3}), D_i is the median diameter and N_i is a function of the kinetic energy flux.

The dust particles are divided into four size bins (or modes): fine (0.01–1.0 μm), accumulation (1.0–2.5 μm), coarse (2.5–5 μm) and giant (5.0–20.0 μm). The dust transport, deposition and removal processes are given by Qian et al. (2001) and Qian and Giorgi (1999):

$$\frac{\partial \chi^i}{\partial t} = -\overline{V} \cdot \nabla \chi^i + F_H^i + F_V^i + F_C^i + S^i - R_{Wls}^i - R_{Wc}^i - D_d^i, \quad (4)$$

where $-\overline{V} \cdot \nabla \chi^i$ is the advection, F_H^i is the horizontal turbulent diffusion, F_V^i is the vertical turbulent diffusion and F_C^i is the convective transport. R_{Wls}^i and R_{Wc}^i are the wet removal terms, represented by large-scale and convective precipitation. D_d^i is the dry deposition, represented by assuming fixed depositional velocities over both land and water.

2.2 Experimental design and observational data

Two numerical experiments were designed; both integrate for 20 years (excluding first two years of spin-up) using the dust-coupled RegCM4.1. The first experiment was a control experiment (CON) that used the default land use types from the Global Land Cover Characterization dataset (Loveland et al., 2000), meaning that dust emitting sources both within and outside the TP. The second experiment was a sensitivity experiment (SEN) where we turned off the dust emission in the northern and northeastern TP (the deserts inside the black outline of the TP contour in Fig. 1b). To eliminate the dust emission in the TP, we replaced the land cover types of these areas with the nearby vegetated types, in a manner similar to the method of Liu et al., (2015a). All the other conditions in the sensitivity experiment were the same as in the control experiment.

The initial and boundary conditions were taken from the NCAR/NCEP re-analysis dataset (Kalnay et al., 1996). The sea surface temperature used the National Oceanic and Atmospheric Administration sea surface temperature dataset (Reynolds et al., 2002). The topography of the TP is very complex, necessitating high spatial resolution (<60 km) to

Atmos. Chem. Phys. Discuss., doi:10.5194/acp-2017-55, 2017
Manuscript under review for journal Atmos. Chem. Phys.
Discussion started: 28 February 2017

Atmospheric Chemistry and Physics Discussions

resolve localized precipitation (Gao et al., 2006). The horizontal resolution in RegCM4.1 runs was therefore set to 40 km. The simulation domain is shown in Fig. 1a and the model domain centered was at (32°N, 105°E), with 240 grid cells in the west–east direction and 160 grid cells in the north–south direction, respectively. The model was run in the standard configuration of 18 vertical σ layers with the model top at 10 hPa. The integration duration for both experiments was from January 1, 1988 to December 31, 2009. The first two years were treated as the model spin-up time and only the results from the last 20 years were analyzed.

Four main types of observations were used to evaluate the simulated results of CON: (1) the monthly mean surface air temperature and precipitation, with a high resolution of 0.5×0.5°, provided by the Climate Research Unit (CRU) of the University of East Anglia (Mitchell and Jones, 2005), which was used to evaluate the simulated surface temperature and precipitation in CON; (2) the NCEP–DOE re-analysis wind field (2.5×2.5°) at 850 hPa, which was used to compare the simulated atmospheric circulation; (3) level-3 monthly mean AOD data from 2000 to 2009 obtained from the Multiangle Imaging Spectroradiometer (MISR) onboard NASA's Earth Observation System Terra satellite (http://www-misr.jpl.nasa.gov/), which was used to evaluate the simulated dust AOD in CON. The effectiveness of the MISR data was investigated by Martonchik et al. (1998, 2004) and was found to perform better than MODIS as a result of its unique design (Prasad and Singh, 2007); and (4) the AOD observed *in situ* by the Aerosol Robotic Network (AERONET), which was used to evaluate the simulated dust seasonal and interannual variation in CON.

3 Results of simulations

In this section we will first evaluate the CON simulation using the observed data described in the previous section. Then the results from CON and SEN experiments will be compared to determine the roles of dust aerosols generated from the TP play in the thermodynamic fields and circulations including the EASM.

3.1 Validation

3.1.1 Basic model climatology

The simulated climatology can influence the distribution of dust aerosols and their climatic effects, so CON was used to analyze the surface temperature, precipitation and atmospheric circulation at 850 hPa. The CON-simulated and CRU-observed 20-year average summer surface temperatures in East Asia are presented respectively in Figs 2a and 2b. The CRU observed temperature is >25°C in southern China, NW China and northern India, and <7°C over the TP. The observed north–south gradient and location of the maximum and minimum centers were captured well by RegCM4.1. The model captured the major distribution patterns of precipitation, including the reasonable SE–NW gradient and the maximum centers in southern China, the Himalaya and Indian Peninsula, with a 2–4 $mmday^{-1}$ negative bias in the Korean Peninsula and south Japan and a 2–4 $mmday^{-1}$ positive bias in the Tianshan Mountains (Figs. 2c, 2d). These simulated deviations are likely related to the cumulus convective scheme in the model (Zhang et al., 2008; Wang and Yu, 2011).

Atmos. Chem. Phys. Discuss., doi:10.5194/acp-2017-55, 2017
Manuscript under review for journal Atmos. Chem. Phys.
Discussion started: 28 February 2017

RegCM4.1 captured the major characteristics of the circulations in East Asia, where southwesterlies dominate to the south side of the TP, and the location of the Indian Low is consistent with the NCEP–DOE observations (Figs. 2e, 2f).

3.1.2 Dust AOD comparison between simulated and MISR observed

Satellite and *in situ* observations include all types of aerosols, such as black aerosols, SO_2 and organic carbon; observed data for dust AOD alone are scarce. Therefore we used the MISR AOD data, as in most previous studies (Zakey et al., 2006; Zhang et al., 2009), to evaluate the spatiotemporal distribution of the dust AOD simulated by the model. Both the simulation and observations showed that the dust AOD over the TP and its surrounding areas was higher in spring and summer (Figs. 3a and 3c) and lower in autumn and winter (Figs. 3e and 3g). There were three maximum centers (maximum value >0.6) of dust AOD in spring and summer, located in the Taklimakan Desert, the Gobi Desert and the Great Indian Desert, respectively. The dust AOD over the Qaidam Basin in the NE of the TP was also >0.5 and the dust AOD over the northern TP, adjacent to the southern Taklimakan Desert, was between 0.3 and 0.5. The simulated dust AOD in these regions was reduced in autumn and winter (Figs. 3e and 3g). The MISR-observed AOD was largely consistent with the model results for the Taklimakan Desert, the Gobi Desert and the Qaidam Basin, but were relatively low in the Great Indian Desert in summer. The large value of the MISR AOD in the Sichuan Basin to the east of the TP was due to industrial emissions, which were not incorporated into our model simulation.

3.1.3 Dust AOD comparison between simulated and AERONET-observed

Figure 4 compares the *in situ* observed monthly mean AOD from AERONET and that simulated by RegCM4.1 at Dalanzadgad (43.6°N, 104.4°E). This is the only available AERONET site in the vicinity of the dust sources with continuous records for >10 years. The model captured the seasonal and interannual variations of AOD well, including the year with extremely high levels of dust. Observations over the TP are scarce and we could only find a site with continuous aerosol records from AERONET at Nam Co (30.77°N, 90.96°E). The seasonal variation of AOD at this site is well captured. Both the simulation and the observations showed that the dust AOD increases in spring at Nam Co (Fig. 5).

3.2 Relationship between the EASM and dust loading over the TP

To study the relationship between dust aerosols and the EASM, we used the average summer meridional wind at 850 hPa over eastern China (20–45°N, 105–122.5°E) as an EASM index, following Xie et al. (2016). This index has been widely used to examine both modern and paleo-changes in the East Asian monsoon (Wang et al., 2008; Jiang and Lang, 2010). We found that the simulated difference in the EASM index (CON−SEN) and the difference in the model-simulated column dust load averaged over the TP are highly anticorrelated with a correlation coefficient R=−0.41 (Fig. 6). The dust aerosol increases and decreases over the TP as the index weakens and enhances respevtively. Lou et al. (2016) also demonstrated a clear negative correlation between the EASM and the dust concentration over eastern China in spring. Based on the variation in the column dust load shown in Fig. 6, we chose 1994 and 2009 as heavy dust years and 2003

and 2007 as light dust years and then contrasted the dust distribution over the TP and its effects on the summer climate in the heavy/light dust years.

3.3 Dust aerosol distribution in heavy/light dust years

In the heavy dust years, the difference in the column dust load over the TP was greater than that in the light dust years, as expected. Two centers of maximum column dust load existed over the TP in the heavy dust years (Fig. 7a). One was located in the Qaidam Basin and the other in the NW of the TP. The maximum values at both centers were >70 mg m^{-2}. However, the difference in the column dust load over the NW of the TP in the light dust years was much lower than in the heavy dust years and the central value was <25 mg m^{-2}. From the vertical profiles of the dust load (Figs 7c and 7d), we can see that the dust mixing ratio was higher in heavy dust years in the western TP with a central value >5 μg kg^{-1}. The mixing ratio was lower in the western TP in the light dust years.

3.4 East Asian climate anomalies in heavy/light dust years induced by dust aerosols

3.4.1 Temperature anomaly

Both the atmospheric heating rate and the atmospheric temperature over the TP decreased in heavy/light dust years (Fig. 8). During the heavy dust years, the dust aerosol resulted in two cooling anomaly centers, one in the lower troposphere (600–400 hPa) over TP core and the other in the upper troposphere (*c.* 300 hPa) of the western TP, with a cooling of >0.4 K day^{-1} due to the large dust load. These cooling anomalies resulted in a low temperature center at 500 hPa over the western TP, with its central value reduced by >0.6°C. The dust aerosol over the TP in the light dust years was much less than in the heavy dust years (Fig. 7a and 7c), so the cooling effect in the light dust years was weaker than in the heavy dust years. The warming to the east of the TP (110–120°E) (Fig. 7c and 7d) is caused by diabatic heating induced by the enhancement of descending motion (figure not shown).

The surface temperature over the TP decreased in both the heavy and light dust years (Fig. 9). In the heavy dust years, the surface temperature decreased by 0.6°C over the TP and the sea–land thermal contrast was reduced. It is worth noting that the effects of TP aerosols on surface temperature were not limited to local or surrounding regions. In fact, the largest impact was in NE China, more than two thousands km downstream (Fig. 9a). The remote cooling is likely contributable to a cold air advection stemmed from the upstream TP aerosols to be discussed in next subsection (Fig. 10).

3.4.2 Circulation

The overall effects of TP aerosols cool the troposphere surrounding the TP (Fig. 9a) and thus the land–sea thermal contrast were reduced by the dust aerosols over the TP. The atmospheric circulation anomaly induced by the dust aerosol emitted over the TP in heavy dust years shows an overall gigantic anticyclonic circulation centered over the TP (Fig. 10a). The northeasterlies that runs against the southwesterly monsoon is especially strong over the EASM region, which

indicates that the EASM was weakened greatly. The anomaly still existed in the light dust years, but its intensity was much weaker than in the heavy dust years (Fig. 10b).

3.4.3 Precipitation

Figure 11 shows the simulated change in summer precipitation in the southern monsoon region of China induced by dust emitted over the TP in heavy and light dust years. The precipitation decreased in the southern monsoon region in summer in the heavy dust years as a result of weakening of the EASM (Fig. 10) and the reduction reached 3 mm day^{-1} in August. The dust aerosol also decreased the precipitation in the light dust years. The simulated suppression effects of the dust aerosol were consistent with previously reported modeling results (Sun et al., 2012; Guo et al., 2015).

3.5 Effects of dust on the onset of the EASM

To analyze the influence of the heating anomalies caused by the dust aerosol emitted over the TP on the onset of EASM, we used the index of EASM onset defined by Wang and Ho (2002):

$$RR_i = R_i - R_{JAN},\quad i = 1,2,\ldots, 73, \tag{5}$$

where RR_i is the relative pentad mean rainfall rate. In the northern hemisphere, R_i is the pentad mean rainfall rate and R_{JAN} is the pentad mean rainfall rate in January. The onset of the EASM occurs when RR_i is >6 mm day^{-1}.

We chose two key monsoon regions of East Asia – a southern monsoon region (22–30°N, 105–120°E) and a northern monsoon region (34–42°E, 105–120°N) – following Liu and Yin (2002). Figure 12 shows that the dust aerosol emitted over the TP delayed the onset of the EASM by one pentad in both the southern and northern monsoon regions.

4 Discussion

Previous research has shown that dust emitted from Asian deserts can weaken the EASM (Sun et al., 2012; Guo et al., 2015; Li et al., 2016), although the details of weakening mechanisms are still unclear. It has been suggested by some authors that the weakening of the EASM is a result of the reduction in the thermal contrast between the land and the sea induced by dust aerosols (Guo and Yin, 2015; Li et al., 2016). However, the modeling result of Sun et al. (2012) showed that the EASM is reduced by the large-scale atmospheric disturbances (cyclone–anticyclone–cyclone Rossby wave train) generated by the radiative cooling of dust aerosols. In the work reported here, we considered the effects of dust aerosols emitted only within the TP itself on regional climate and found that they can also reduce the EASM significantly by weakening the heat source ("pump") over the TP and thus reduce the land–sea thermal contrast. The locally generated TP dust can cause surface cooling far downstream in eastern Mongolia and northeastern China through stationery Rossby wave propagation. The dust-loading over the TP include both local emissions and external sources; our sensitivity simulations showed there was a negative correlation between the EASM and dust aerosols emitted from the TP locally.

It is worth noting that Sun and Liu (2016) demonstrated that dust emitted from Taklimakan and Gobi Deserts weakens the Asian monsoon through large-scale atmospheric disturbances by 2 m s^{-1} of wind at 700 hPa. This magnitude of reduction in the wind seems small compared to the values in the present study even though the emission source extent in the previous is larger. We think both high-altitude source like the TP and low-altitude sources such as Taklimakan and Gobi Desert can weaken the EASM, but the mechanism could differ. The dust emitted from low altitude source (mainly Taklimakan and Gobi Desert) reduces the EASM mainly by the large-scale atmospheric disturbances, while the dust emitted from high-altitude source weakens the EASM by the reduction in the TP heating and in thermal contrast in the middle troposphere between the land and sea. The column dust load induced by local emissions from the TP in heavy dust years accounted for 20% ((CON−SEN)/CON) of the total loading over the TP, its impacts on Asian monsoon and climate seems more important than the low altitude sources such as Taklimakan and Gobi Desert in East Asia. This disproportionately large impact from TP locally emitted dust is likely due to its higher elevation within TP itself so that the dust-induced cooling can more effectively weaken the TP's acting as a heat pump for the Asian monsoon. Further studies on this is rightly warranted.

Only direct radiative effects of dust were included in our model and future studies should include both direct and indirect effects. The simulated effects of dust aerosols on climate were highly sensitive to the physical characteristics of the dust aerosols, such as the single scattering albedo (Huang et al., 2014; Colarco et al., 2014; Das et al., 2015). Therefore our results also need to be validated by sensitivity experiments using aerosols with different properties. In addition, many other factors can also affect the EASM, including the El Niño Southern Oscillation (Zhao et al., 2012; Liu et al., 2015b), the North Atlantic Oscillation (Wu et al., 2009) and heat sources over the TP (Yanai and Wu, 2006; Duan et al., 2012). A recent numerical simulation by Wang et al. (2017) showed that aerosol emissions from outside East Asian play an important part in weakening the circulation of the EASM.

5 Conclusions

We conducted two numerical experiments to quantify the effects of dust aerosols emitted over the TP on the EASM in heavy/light dust years using a high-resolution regional climate model. Satellite and *in situ* observations were used to evaluate the simulated spatial distribution of dust aerosols and their seasonal and interannual variations. We analyzed the change in dust aerosols induced by emissions over the TP and their radiative effects on the EASM and summer precipitation in heavy/light dust years. We also studied the effects of dust aerosols on the onset of the EASM.

The spatiotemporal distribution of the dust AOD and their seasonal and interannual variation were captured well by the RegCM4.1 model compared with the MISR AOD and *in situ* observations from AERONET. Both the simulated and observed AOD were higher in spring/summer and lower in autumn/winter. The simulated dust AOD was higher in the Taklimakan Desert, the Gobi Desert and the Great Indian Desert, with peak values >0.6. The simulated dust AOD in the

Qaidam Basin and the northern TP were also higher. The seasonal variation in the dust AOD at Nam Co was captured well by RegCM4.1 relative to the observed aerosol AOD.

Comparative analyses of the two simulations indicated that the dust aerosols generated over the TP had a profound influence on the EASM. The difference in the EASM index and column dust load between CON and SEN experiments are negatively correlated (R=−0.41). The index also weakened (enhanced) as the imported-local combined dust aerosol increased (decreased) over the TP. The net atmospheric heating rate was negative over the TP in heavy dust years as a result of the radiative cooling effects of the dust aerosols, leading to a 0.6°C cooling in the surface and atmospheric temperatures. The land–sea thermal contrast and EASM were therefore both weakened, causing a 12% reduction in precipitation in the southern monsoon region. The dust load over the TP in the light dust years was much less than in the heavy dust years, implying large interannual variability. The dust aerosols produced over the TP can delay the onset of the EASM by one pentad in both the northern and southern monsoon regions of China.

Acknowledgements. This research was jointly supported by the National Key Research and Development Program of China (2016YFA0601904), the National Natural Science Foundation of China (41405093, 41572150, 41475085).

References

Alfaro, S. C. and Gomes, L.: Modeling mineral aerosol production by wind erosion: Emission intensities and aerosol size distributions in source areas, J. Geophys. Res., 106(D16), 18075–18084, doi:10.1029/2000JD900339, 2001.

Anthes, R. A.: A cumulus parameterization scheme utilizing a one-dimensional cloud model, Mon. Weather Rev., 105, 270–286, doi: http://dx.doi.org/10.1175/1520-0493(1977)105<0270:ACPSUA>2.0.CO;2, 1977.

Chen, S. Y., Huang, J. P., Zhao, C., Qian, Y., Leung, R., and Yang, B.: Modeling the transport and radiative forcing of Taklimakan dust over the Tibetan Plateau: A case study in the summer of 2006, J. Geophys. Res., 118, 797–812, doi: 10.1002/jgrd.50122, 2013.

Chin, M., Ginoux, P., Kinne, S., Torres, O., Holben, B. N., Duncan, B. N., Martin, R. V., Logan, J. A., Higurashi, A., and Nakajima, T.: Tropospheric aerosol optical thickness from the GCART model and comparisons with satellite and Sun photometer measurements, J. Atmos. Sci., 59, 461–483, doi: http://dx.doi.org/10.1175/1520-0469(2002)059<0461:TAOTFT>2.0.CO;2, 2002.

Colarco, P. R., Nowottnick, E. P., Randles, C. A., Yi, B. Q., Yang, P., Kim, K. M., Smith, J. A., and Bardeen, C. G.: Impact of radiatively interactive dust aerosols in the NASA GEOS-5 climate model: sensitivity to dust particle shape and refractive index, J. Geophys. Res., 119(2), 753–786, doi: 10.1002/2013JD020046, 2014.

Das, S., Dey, S., Dash, S. K., Giuliani, G., and Solmon, F.: Dust aerosol feedback on the Indian summer monsoon: Sensitivity to absorption property, J. Geophys. Res., 120, 9642–9652, doi: 10.1002/2015JD023589, 2015.

Dickinson, R. E., Henderson-Sellers, A., and Kennedy, P. J.: Biosphere-atmosphere transfer scheme (bats) version 1e as coupled to the NCAR community climate model, NCAR Tech., National Center for Atmospheric Research Technical Note No. TN-387+STR, NCAR, Boulder, CO, 1993.

Duan, A., Wu, G., Liu, Y., Ma, Y., and Zhao, P.: Weather and climate effects of the Tibetan Plateau, Adv. Atmos. Sci., 29, 78–992, doi: 10.1007/s00376-012-1220-y, 2012.

Emanuel, K. A.: A scheme for representing cumulus convection in large-scale models, J. Atmos. Sci., 48(21), 2313–2335, doi: 10.1175/1520-0469(1991)048<2313:ASFRCC>2.0.CO;2, 1991.

Fang, X. M.: The origin and provenance of the Malan loess along the eastern margin of the Qinhai-Xizang (Tibetan) Plateau and its adjacent area, Sci. China SER B, 38(7), 876–887, 1995.

Fang, X. M., Li, J. J., and Van der Voo, R.: Rock magnetic and grain size evidence for intensified Asian atmospheric circulation since 800 kyrs BP to Tibetan uplift. Earth Planet, Sc. Lett., 165, 129–144, doi: http://dx.doi.org/10.1016/S0012-821X(98)00259-3, 1999.

Fecan, F., Marticorena, B., and Bergametti, G.: Parameterization of the increase of aeolian erosion threshold wind friction velocity due to soil moisture for arid and semi-arid areas, Ann. Geophys., 17, 149–157, doi: 10.1007/s00585-999-0149-7, 1999.

Gao, X. J., Xu, Y., Zhao, Z. C, Pal, J. S., and Giorgi, F.: On the role of resolution and topography in the simulation of East Asia precipitation, Theor. Appl. Climatol., 86, 173–185, doi: 10.1007/s00704-005-0214-4, 2006.

Giorgi. F., Coppola, E., Solmon, F., Mariotti, L., Sylla, M. B., Bi, X., Elguindi, N., Diro, G. T., Nair, V., Giuliani, G., Turuncoglu, U. U., Cozzini, S., Güttler, I., O'Brien, T. A., Tawfik, A. B., Shalaby., Zakey, A. S., Steiner, A. L., Stordal, F., Sloan, L. C., and Brankovic, C.: RegCM4: Model description and preliminary tests over multiple CORDEX domains, Clim. Res., 52, 7–29, doi: 10.3354/cr01018, 2012.

Goudie, A. S.: Dust storms in space and time, Prog. Phys. Geog., 7, 502–530, doi: 10.1177/030913338300700402, 1983.

Grell, G. A., Dudhia, J., and Stauffer, D. R.: Description of the fifth generation Penn State/NCAR Mesoscale Model (MM5), National Center for Atmospheric Research Technical Note No. TN-398+STR, NCAR, Boulder, Colo, 1994.

Grell, G. A.: Prognostic evaluation of assumptions used by cumulu parameterizations, Mon. Weather Rev., 121, 764–787, doi: 10.1175/1520-0493(1993)121<0764:PEOAUB>2.0.CO;2, 1993.

Guo, J. and Yin, Y.: Mineral dust impacts on regional precipitation and summer circulation in East Asia using a regional coupled climate system model, J. Geophys. Res., 120, 10378–10398, doi: 10.1002/2015JD023096, 2015.

Holtslag, A., De Bruijn, E., and Pan, H. L.: A high resolution air mass transformation model for short-range weather forecasting, Mon. Weather Rev., 118(8), 1561–1575, doi: 10.1175/1520-0493(1990)118<1561:AHRAMT>2.0.CO;2, 1990.

Huang, J. P., Minnis, P., Yi, Y. H., Tang, Q., Wang, X., Hu, Y. X., Liu, Z. Y., Ayers, K., Trepte, C., and Winker, D.: Summer dust aerosols detected from CALIPSO over the Tibetan Plateau, Geophys. Res. Lett., 34, L18805, doi:10.1029/2007GL029938, 2007.

Huang, J. P., Fu, Q., Su, J., Tang, Q., Minnis, P., Hu, Y., Yi, Y., and Zhao Q.: Taklimakan dust aerosol radiative heating derived from CALIPSO observations using the Fu-Liou radiation model with CERES constraints, Atmos. Chem. Phys., 9, 4011–4021, doi: 10.5194/acp-9-4011-2009, 2009.

Huang, J. P., Wang, T., Wang, W., Li, Z., and Yan, H.: Climate effects of dust aerosols over East Asian arid and semiarid regions, J. Geophys. Res., 110, 11398–11416, doi: 10.1002/2014JD021796, 2014.

Jia, R., Liu, Y., Chen, B., Zhang, Z., and Huang, J.: Source and transportation of summer dust over the Tibetan Plateau, Atmos. Environ., 123, 210–219, doi: 10.1016/j. atmosenv.2015.10.038, 2015.

Jiang, D. B. and Lang, X. M.: Last Glacial Maximum East Asian monsoon: Results of PMIP simulations, J. Clim., 23, 5030–5038, doi: 10.1175/2010JCLI3526.1, 2010.

Kalnay, E., Kanamitsu, M., Kistler, R., Collins, W. G., Deaver, D., Gandin, L. S., Iredell, M., Saha, S., White, G., Woollen, J., Zhu, Y., Chelliah, M., Ebisuzaki, W., Higgins, W., Janowiak, J. E., Mo, K., Ropelewski, C., Wang, J. L., and Leetmaa, A.: The NCEP/NCAR 40-year reanalysis project, Bull. Am. Meteorol. Soc., 77, 437–471, doi: http://dx.doi.org/10.1175/1520-0477(1996)077<0437:TNYRP>2.0.CO;2, 1996.

Kiehl, J., Hack, J., Bonan, G., Boville, B., Breigleb, B., Williamson, D., and Rasch, P.: Description of the NCAR community climate model (CCM3). National Center for Atmospheric Research Technical Note No. NACR/TN-420+STR, NCAR, Boulder, CO, 1996.

Lau, K. M., Kim, M. K, and Kim, K. M.: Asian monsoon anomalies induced by aerosol direct forcing: the role of the Tibetan Plateau, Clim. Dyn., 26, 855–64, doi: 10.1007/s00382-006-0114-z, 2006.

Lau, K. M., Kim, M. K., Kim, K. M., and Lee, W. S.: Enhanced surface warming and accelerated snow melt in the Himalayas and Tibetan Plateau induced by absorbing aerosols, Environe. Res. Lett., 5, 025204, doi: 10.1088/1748-9326/5/2/025204, 2010.

Li, S., Wang, T. J, Solmon, F., Zhuang, B. L., Wu, H., Xie, M., Han, Y., and Wang, X. M.: Impact of aerosols on regional climate in southern and northern China during strong/weak East Asian summer monsoon years, J. Geophys. Res., 121, 4069–4081, doi: 10.1002/2015JD023892, 2016.

Liu, X. D. Yin, Z. Y.: Sensitivity of East Asian monsoon climate to the Tibetan Plateau, Palaeogeogr. Palaeocl., 183, 223–245, doi: 10.1016/S0031-0182(01)00488-6, 2002

Liu, X. D., Sun, H., Miao, Y. F., Dong, B. W., and Yin, Z. Y.: Impact of uplift of northern Tibetan Plateau and formation of Asian inland deserts on regional climate and environment, Quaternary Sci Rev., 116, 1–14, doi: 10.1016/j.quascirev.2015.03.010, 2015a.

Liu, Y. Y., Hu, Z. Z., Kumar, A., Peng, P., Collins, D. C., and Jha, B.: Tropospheric biennial oscillation of summer monsoon rainfall over East Asia and its association with ENSO, Clim. Dyn., 45, 1747–1759, doi: 10.1007/s00382-014-2429-5, 2015b.

Loveland, T. R., Reed, B. C., Brown, J. F., Ohlen, D. O., Zhu, Z., Yang, L., and Merchant, J. W.: Development of a global land cover characteristic database and IGBP DISCover from 1-km AVHRR data, Int. J. Remote Sens., 21(6), 1303–1330, doi: https://doi.org/10.1080/014311600210191, 2000.

Lou, S., Russell, L. M., Yang, Y., Xu, L., Lamjiri, M. A., DeFlorio, M. J., Miller, A. J., Ghan, S. J., Liu, Y., and Singh, B.: Impacts of the East Asian Monsoon on springtime dust concentrations over China, J. Geophys. Res., 121, 8137–8152, doi:10.1002/2016JD024758, 2016.

Marticorena, B. and Bergametti, G.: Modeling the atmospheric dust cycle: 1. Design of a soil-derived dust emission scheme, J. Geophys. Res., 100(D8), 16415–16430, 1995.

Martonchik, J. V., Diner, D. J., Kahn, R. A., Ackerman, T. P., Verstraete, M. E., Pinty, B., and Gordon, H. R.: Techniques for the retrieval of aerosol properties over land and ocean using multiangle imaging, IEEE Trans. Geosci. Remote Sens., 36(4), 1212–1227, 1998.

Martonchik, J. V., Diner, D. J., Kahn, R., Gaitley, B., and Holben, B. N.: Comparison of MISR and AERONET aerosol optical depths over desert sites, Geophys. Res. Lett., 31, L16102, doi: 10.1029/2004GL019807, 2004.

Miller, R. L., Perlwitz, J., and Tegen, I.: Modeling Arabian dust mobilization during the Asian summer monsoon: The effect of prescribed versus calculated SST, Geophys. Res. Lett., 31(22), 519–540, doi: 10.1029/2004GL020669, 2004.

Mitchell, T. D. and Jones, P. D.: An improved method of constructing a database of monthly climate observations and associated high-resolution grids, Int. J. Climatol., 25, 693–712, doi: 10.1002/joc.1181, 2005.

Oleson, K. W., Niu, G. Y., Yang, Z. L., Lawrence, D. M., Thornton, P. E., Lawrence, P. J., Stockli, R., Dickinson, R. E., Bonan, G. B., Levis, S., Dai, A., and Qian, T.: Improvements of the Community Land Model and their impact on the Hydrological cycle, J. Geophys. Res., 113, 811–827, doi:10.1029/2007JG000563, 2008.

Park, S. S. and Kim, Y. J.: Source contributions to fine particulate matter in an urban atmosphere, Chemosphere, 59(2), 217–226, doi: 10.1013/j.chemosphere.2004.11.001, 2005.

Prasad, A. K. and Singh, R. P.: Comparison of MISR-MODIS aerosol optical depth over the Indo-Gangetic basin during the winter and summer seasons (2000–2005), Remote Sens. Environ., 107(1–2), 109–119, doi: 10.1013/j.rse. 2006.09.026, 2007.

Qian, Y. and Giorgi, F.: Interactive coupling of regional climate and sulfate aerosol models over East Asia, J. Geophys. Res., 104, 6477–6499, doi:10.1029/98JD02347, 1999.

Qian, Y., Giorgi, F. Huang, Y. Chameides, W. and Luo C.: Regional simulation of anthropogenic sulfur over East Asia and its sensitivity to model parameters, Tellus B, 53, 171–191, doi:10.1034/j.1600-0889.2001.d01-14.x, 2001.

Qian, Y., Leung, L. R., Ghan, S. J., and Giorgi, F.: Regional climate effects of aerosols over China: Modeling and observation, Tellus B, 55(4), 914–934, doi: doi: 10.1046/j.1435-6935.2003.00070.x, 2003.

Reynolds, R. W., Rayner, N. A., Smith, T. M., Stokes, D. C., and Wang, W. Q.: An improved in situ and satellite SST analysis for climate, J. Clim., 15, 1609–1625, doi: 10.1175/1520-0442(2002)015, 2002.

Rosenfeld, D., Rudich, Y., and Lahav, R.: Desert dust suppressing precipitation: A possible desertification loop, Proc. Natl. Acad. Sci. USA, 98(11), 5975–5980, doi: 10.1073/pnas.101122798, 2001

Solmon, F., Mallet, M., Elguindi, N., Giorgi, F., Zakey, A., and Konaré, A.: Dust aerosol impact on regional precipitation over western Africa, mechanisms and sensitivity to absorption properties, Geophys. Res. Lett., 35, L24705, doi: 10.1029/2008GL035900, 2008.

Sun, H., Pan, Z. T., and Liu, X. D.: Numerical simulation of spatial-temporal distribution of dust aerosol and its direct radiative effects on East Asian climate, J. Geophys. Res., 117(D13), 110–117, doi: 10.1029/2011JD017219, 2012.

Sun, H. and Liu, X. D.: Numerical modeling of topography-modulated dust aerosol distribution and its influence on the onset of East Asian summer monsoon, Adv. Meteorol., 2016(4), 1–15, doi: 10.1155/2016/6951942, 2016.

Tegen, I. and Lacis, A. A.: Modeling of particle size distribution and its influence on the radiative properties of mineral dust aerosol, J. Geophys. Res., 101(D14), 19237–19244, doi: 10.1029/95JD03610, 1996.

Uno, I., Eguchi, K., Yumimoto, K., Takemura, T., Shimizu, A., Uematsu, M., Liu, Z., Wang, Z., Hara, Y., and Sugimoto, N.: Asian dust transported one full circuit around the globe, Nat. Geosci., 2, 557–560, doi:10.1038/ngeo583, 2009.

Wang, B. and Ho, L.: Rainy season of the Asian-Pacific summer monsoon, J. Clim., 15(4), 386–398, doi: 10.1175/1520-0442(2002)015<0386:RSOTAP>2.0.CO;2, 2002.

Wang, B., Wu, Z., Li, J., Liu, J., Chang, C. P., Ding, Y., and Wu, G.: How to measure the strength of the East Asian summer monsoon, J. Clim., 21, 4449–4463, doi: 10.1175/2008JCLI2183.1, 2008.

Wang, C. T. and Yu, L.: Sensitivity of regional climate model to different cumulus parameterization schemes in simulation of the Tibetan Plateau climate, Chin. J. Atmos. Sci., 35(6), 1132–1144 (Chinese), 2011.

Wang, Q. Y., Zhang, Z. L., and Zhang, H.: Impact of anthropogenic aerosols from global, East Asian, and non-East Asian sources on East Asian summer monsoon system, Atmos. Res., 183, 224–236, doi: 10.1016/j.atmosres.2016.08.023, 2017.

Wang, Y. Q., Zhang, X. Y., Gong, S. L., Zhou, C. H., Hu, X. Q., Liu, H. L., Niu, T., and Yang, Y. Q.: Surface observation of sand and dust storm in East Asia and its application in CUACE/Dust, Atmos. Chem. Phys., 8, 545–553, 2008.

Wu, G., Liu, Y., He, B., Bao, Q., Duan, A., and Jin, F. F.: Thermal controls on the Asian summer monsoon, Sci. Rep., 2, 404, doi: 10.1038/srep00404, 2012.

Wu, Z., Wang, B., Li, J., and Jin, F. F.: An empirical seasonal predication model of the east Asian summer monsoon using ENSO and NAO, J. Geophys. Res., 114(D18), 85–86, doi: 10.1029/2009JD011733, 2009.

Xie, X., Wang, H., Liu, X., Li, J., Wang, Z., and Liu, Y.: Distinct effects of anthropogenic aerosols on the effect Asian summer monsoon between multidecadal strong and weak monsoon stages, J. Geophys. Res., 121, doi: doi:10.1002/2015JD024228, 2016.

Yanai, M., Wu, G. X., and Wang, B.: Effects of the Tibetan Plateau In The Asian Monsoon, Springer, Berlin, 513–549, 2006.

Zakey, A. S., Solmon, F., and Giorgi, F.: Implementation and testing of a desert dust module in a regional climate model, Atmos. Chem. Phys., 6, 4687–4704, doi:10.5194/acp-6-4687-2006, 2006.

Zhang, X. Y., Zhang, G. Y., Zhu, G. H., Zhang, D. R., An, Z. S., and Chen, T., Huang, X. P.: Elemental tracers for Chinese source dust, Sci. China SER D, 39(5), 512–521, 1996.

Zhang, D. F., Gao, X. J., Ouyang, L. C., and Dong, W. J.: Simulation of present climate over East Asia by a regional climate model, J. Trop. Meteorol., 14, 19–23, 2008.

Zhang, D. F., Zakey, A. S, Gao, X. J., Giorgi, F., and Solmon, F.: Simulation of dust aerosol and its regional feedbacks over East Asia using a regional climate model, Atmos. Chem. Phys., 9, 1095–1110, doi:10.5194/acp-9-1095-2009, 2009.

Zhao, T. L., Gong, S. L., Zhang, X. Y., Blanchet, J. P., Mckendry, I. G., and Zhou Z. J.: A simulated climatology of Asian dust aerosol and its trans-pacific transport. Part I: mean climate and validation, J. Clim., 19(1), 104–122, doi: 10.1175/JCLI3606.1, 2006

Zhao, T. L., Gong, S. L., Huang, P., and Lavoue D.: Hemispheric transport and influence of meteorology on global aerosol climatology, Atmos. Chem. Phys., 12, 7609–7624, doi: 10.5194/acp-12-7609-2012, 2012.

Atmos. Chem. Phys. Discuss., doi:10.5194/acp-2017-55, 2017
Manuscript under review for journal Atmos. Chem. Phys.
Discussion started: 28 February 2017

Atmospheric Chemistry and Physics Discussions

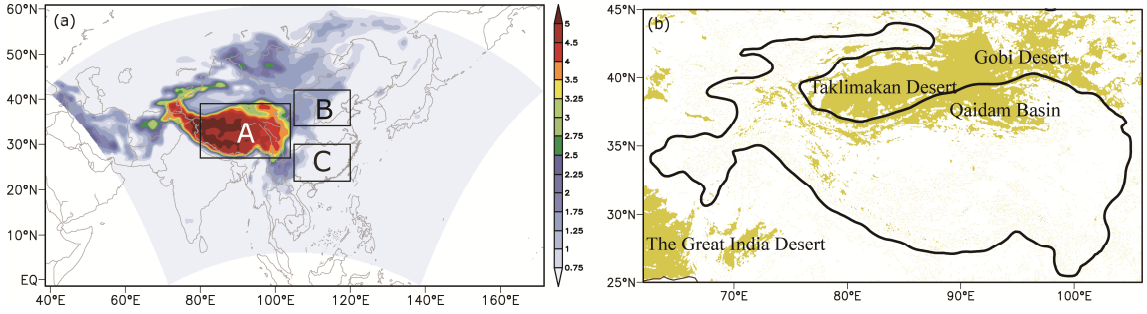

Figure 1: (a) Model domain and topography (units: km) and (b) dust source regions (yellow area) over the Tibetan Plateau and surrounding areas. Rectangles in (a) indicate areas Tibetan Plateau (A, 27–39°N, 80–105°E), north EASM region (B, 34–42°N, 105–120°E), and south EASM region (C, 22–30°E, 105–120°N).

Atmos. Chem. Phys. Discuss., doi:10.5194/acp-2017-55, 2017
Manuscript under review for journal Atmos. Chem. Phys.
Discussion started: 28 February 2017

Atmospheric Chemistry and Physics Discussions

5

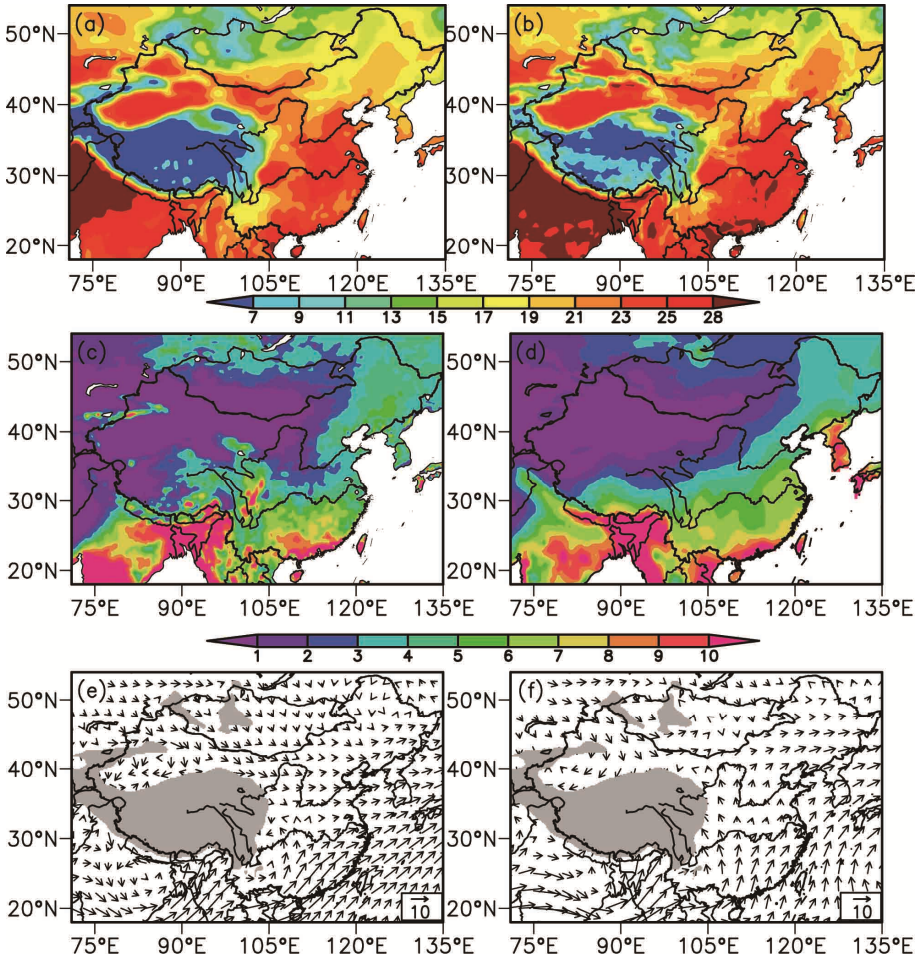

Figure 2: Spatial distribution of (a, b) surface air temperature (°C) and (c, d) precipitation (mm day^{-1}) simulated in the control experiment (left) and the CRU observations (right) for 1990–2009. The bottom two panels are wind vectors at 850 hPa simulated in (e) the control experiment and (f) the NCEP–DOE re-analysis during the summer monsoon season (June–August) averaged for 1990–2009.

Atmos. Chem. Phys. Discuss., doi:10.5194/acp-2017-55, 2017
Manuscript under review for journal Atmos. Chem. Phys.
Discussion started: 28 February 2017

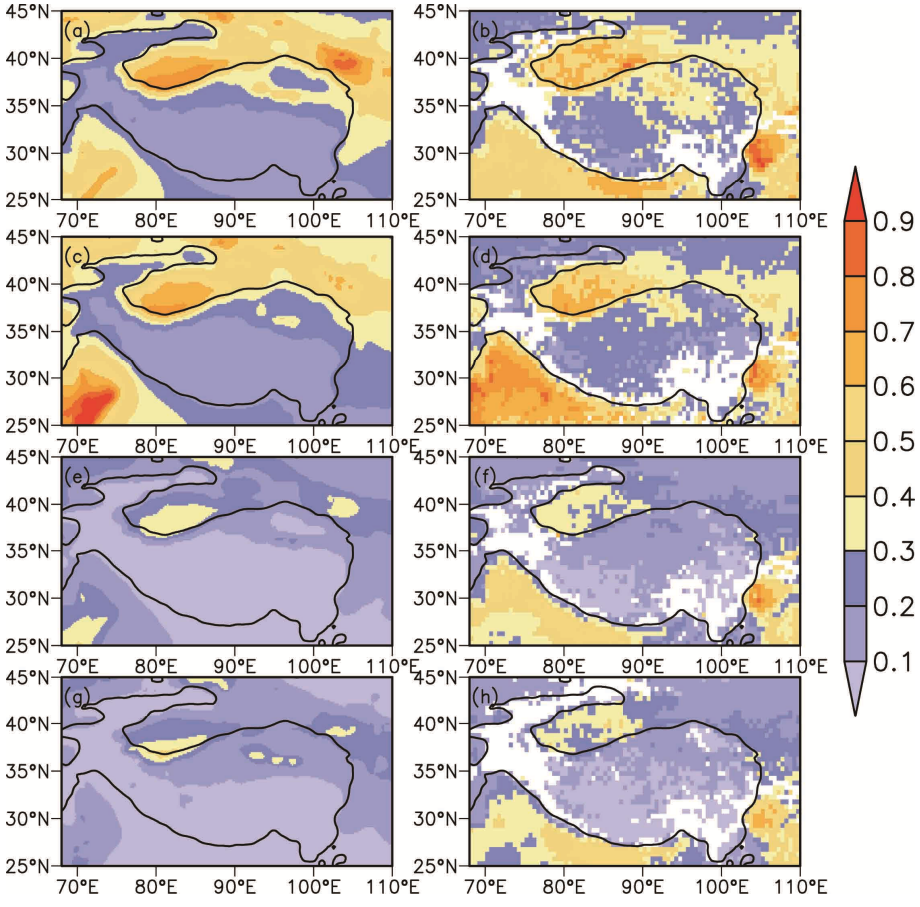

Figure 3: Spatial distribution of the dust AOD simulated by the control experiment (left panels) and the total aerosol optical depth observed by MISR at 550 nm (right panels) averaged in (a, b) spring, (c, d) summer, (e, f) autumn and (g, h) winter during the time period 2000–2009.

Atmos. Chem. Phys. Discuss., doi:10.5194/acp-2017-55, 2017
Manuscript under review for journal Atmos. Chem. Phys.
Discussion started: 28 February 2017

Atmospheric Chemistry and Physics Discussions

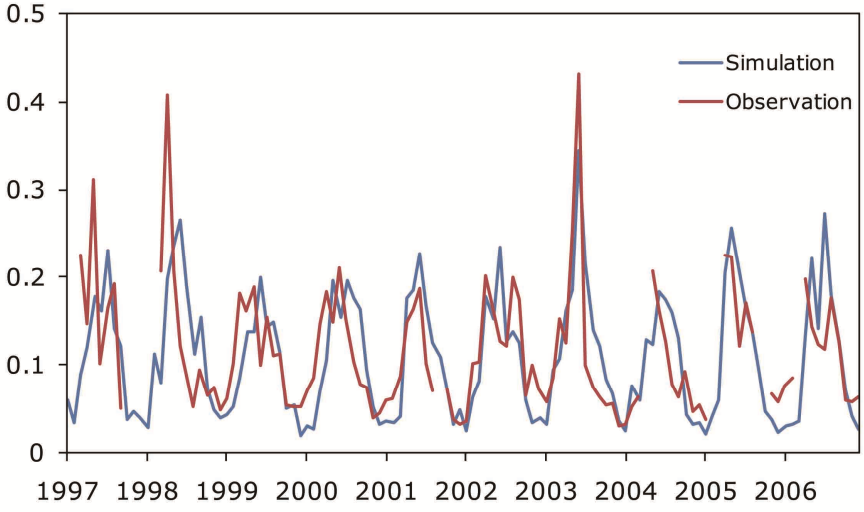

Figure 4: Comparison between the simulated variation of the monthly mean dust AOD in the control experiment and the AERONET-observed variation of the monthly mean aerosol AOD (500 nm) at Dalanzadgad from 1997 to 2006.

Atmos. Chem. Phys. Discuss., doi:10.5194/acp-2017-55, 2017
Manuscript under review for journal Atmos. Chem. Phys.
Discussion started: 28 February 2017

Atmospheric Chemistry and Physics Discussions

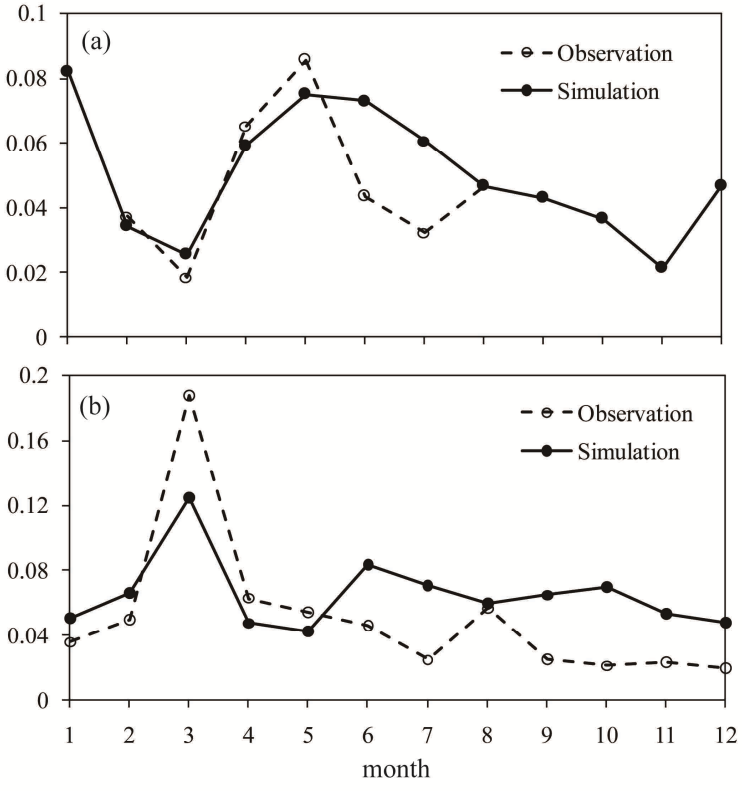

Figure 5: Comparison between the AERONET-observed monthly mean aerosol AOD (500 nm) at Nam Co and simulated by the control experiment at the grid near Nam Co in (a) 2007 and (b) 2009.

Atmos. Chem. Phys. Discuss., doi:10.5194/acp-2017-55, 2017
Manuscript under review for journal Atmos. Chem. Phys.
Discussion started: 28 February 2017

Atmospheric Chemistry and Physics Discussions

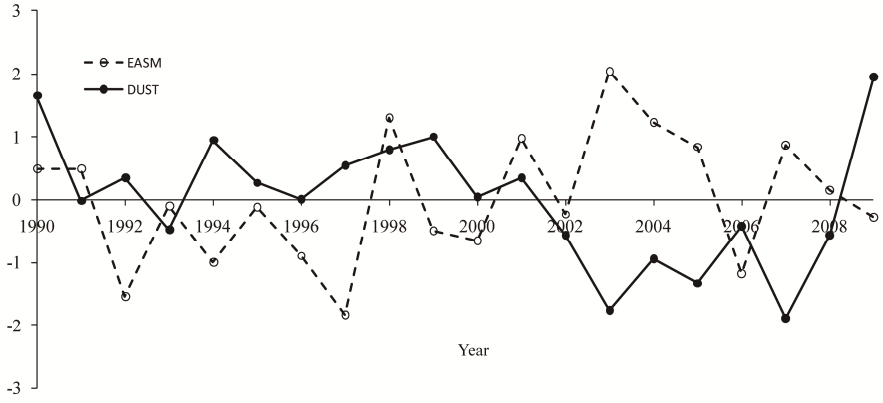

Figure 6: Difference (CON minus SEN) in the normalized regional mean dust column load averaged over the Tibetan Plateau (27–39°N, 80–105°E) and in the EASM index for summer during the period 1990–2009 (R=−0.41).

Atmos. Chem. Phys. Discuss., doi:10.5194/acp-2017-55, 2017
Manuscript under review for journal Atmos. Chem. Phys.
Discussion started: 28 February 2017

Atmospheric Chemistry and Physics Discussions

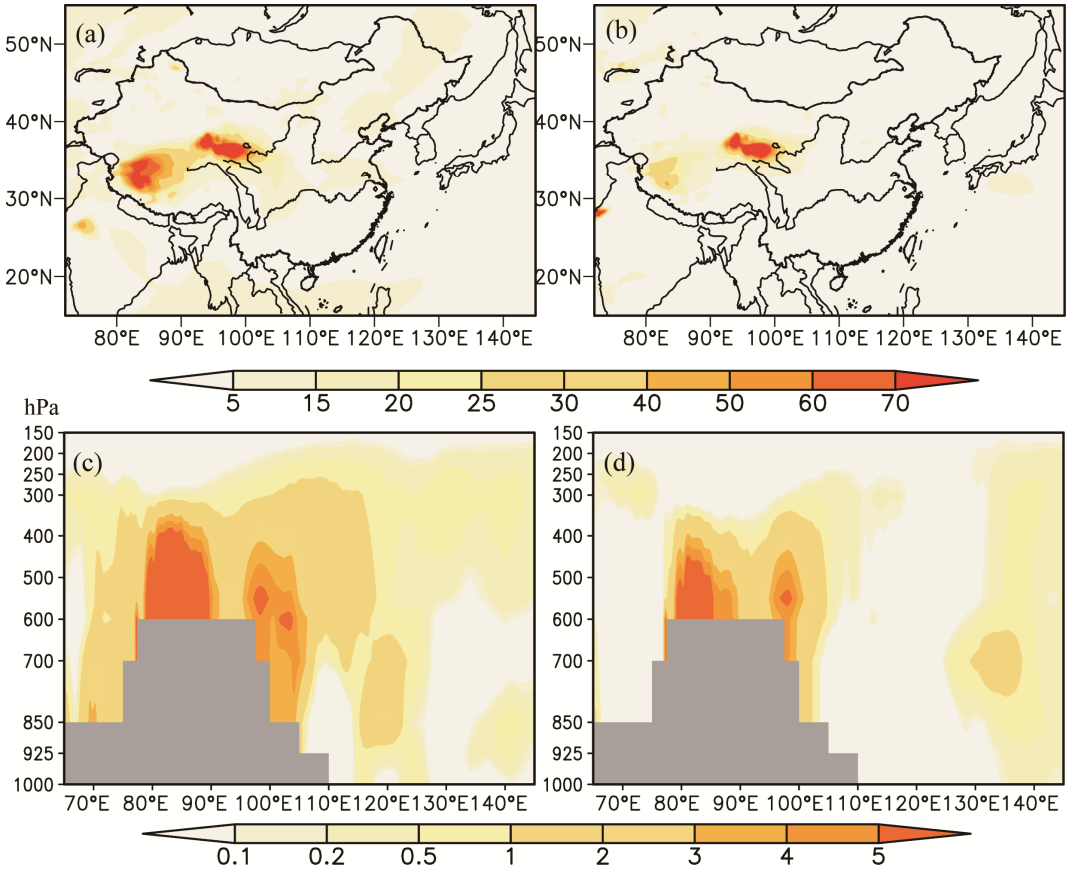

Figure 7: (a, b) Simulated differences (CON minus SEN) in the horizontal distribution of the column dust load (mg m^{-2}) and (c, d) the longitude–height cross-section (averaged over 32–36°N) of the dust mixing ratio (μg kg^{-1}) for summer in heavy (left) and light dust years (right).

Atmos. Chem. Phys. Discuss., doi:10.5194/acp-2017-55, 2017
Manuscript under review for journal Atmos. Chem. Phys.
Discussion started: 28 February 2017

Atmospheric Chemistry and Physics Discussions

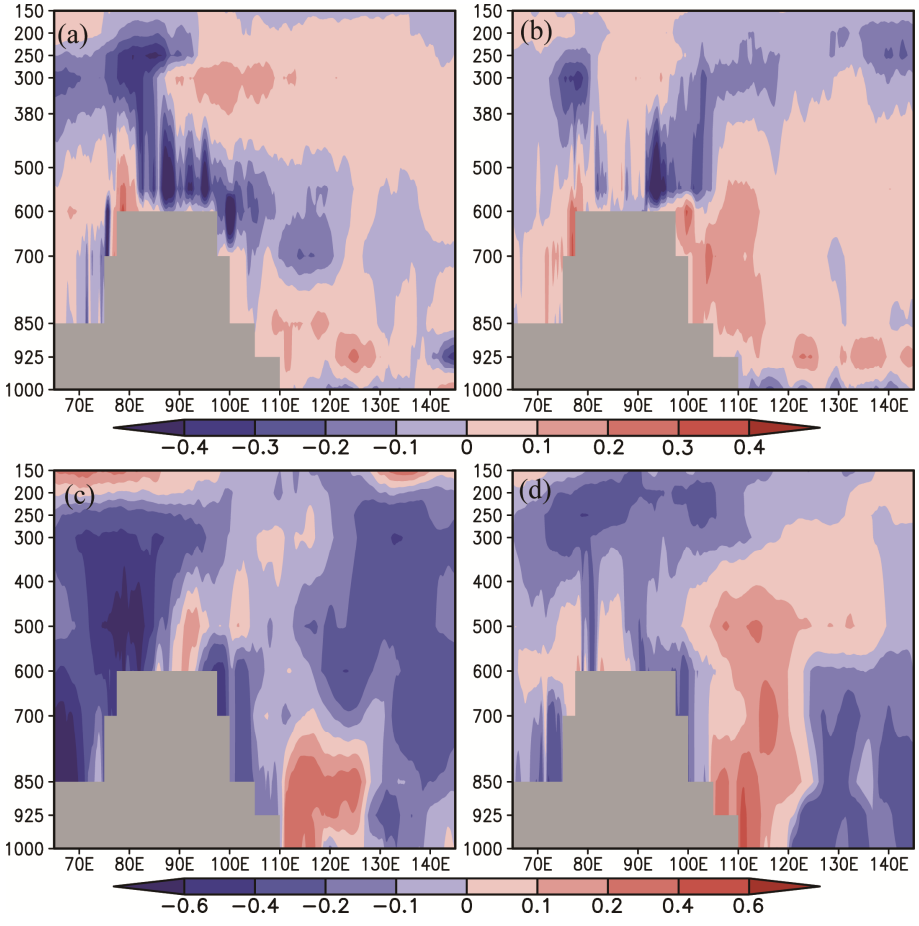

Figure 8: Longitudional cross-section of the differences between CON and SEN averaged over 32–36°N in summer. (a) and (b): net radiative cooling rate (short-wave heating rate + long-wave cooling rate, K day^{-1}) in heavy and light dust years respectively. (c) and (d): as (a) and (b) but for atmospheric temperature.

Atmos. Chem. Phys. Discuss., doi:10.5194/acp-2017-55, 2017
Manuscript under review for journal Atmos. Chem. Phys.
Discussion started: 28 February 2017

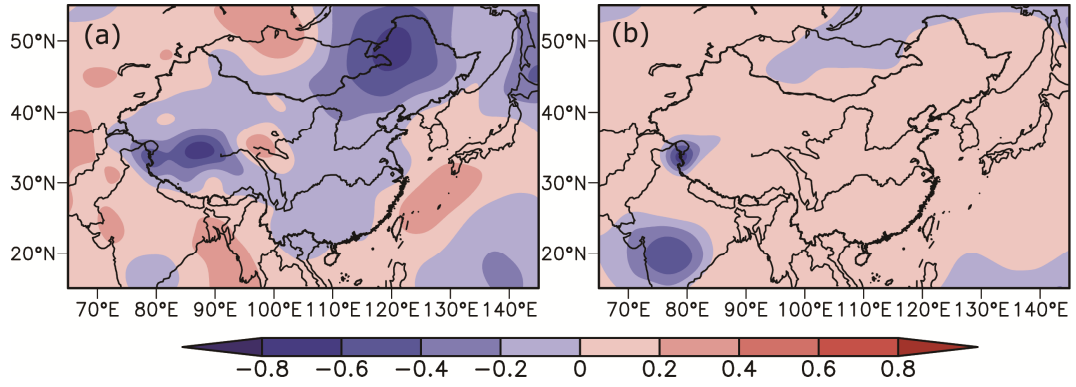

Figure 9: Simulated difference in summer surface temperature between CON and SEN in (a) heavy and (b) light dust years.

Atmos. Chem. Phys. Discuss., doi:10.5194/acp-2017-55, 2017
Manuscript under review for journal Atmos. Chem. Phys.
Discussion started: 28 February 2017

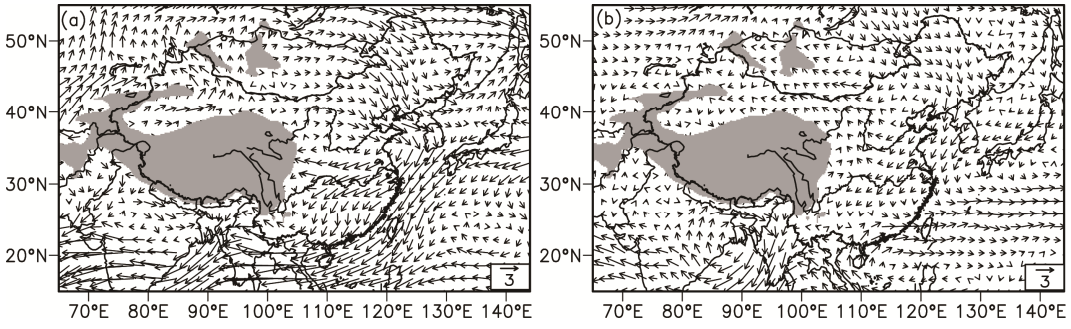

Figure 10: Simulated difference in atmospheric circulation at 850 hPa in summer (m s^{-1}) between CON and SEN in (a) heavy and (b) light dust years.

Atmos. Chem. Phys. Discuss., doi:10.5194/acp-2017-55, 2017
Manuscript under review for journal Atmos. Chem. Phys.
Discussion started: 28 February 2017

Atmospheric Chemistry and Physics Discussions

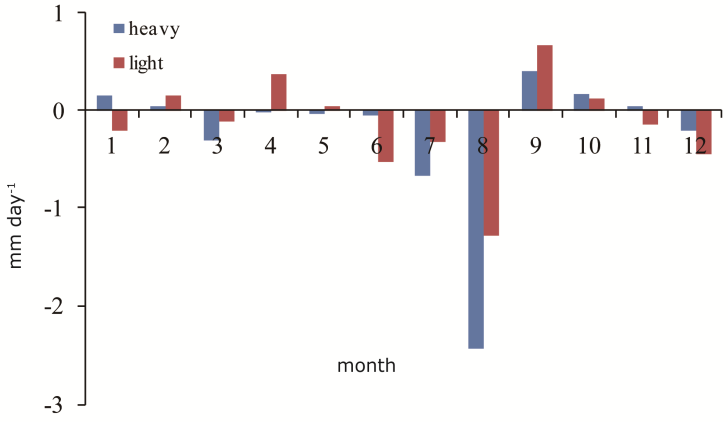

Figure 11: Simulated annual cycle of the regional average monthly precipitation difference (mm day^{-1}) between CON and SEN in heavy and light dust years for the southern monsoon region of China (22–30°E, 105–120°N).

Atmos. Chem. Phys. Discuss., doi:10.5194/acp-2017-55, 2017
Manuscript under review for journal Atmos. Chem. Phys.
Discussion started: 28 February 2017

Atmospheric Chemistry and Physics Discussions

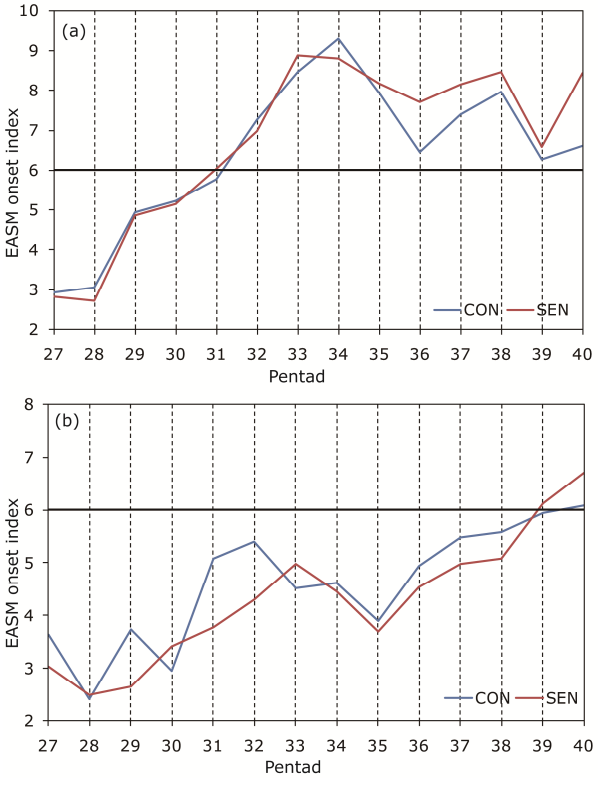

Figure 12. Differences in the EASM index averaged in (a) the southern monsoon region (22–30°E, 105–120°N) and (b) the northern monsoon region (34–42°N, 105–120°E).